

UC San Diego

UC San Diego Previously Published Works

Title

Antitumor activity of an anti-CD98 antibody.

Permalink

<https://escholarship.org/uc/item/2zv479w2>

Journal

International journal of cancer, 137(3)

ISSN

0020-7136

Authors

Hayes, Gregory M
Chinn, Lawrence
Cantor, Joseph M
[et al.](#)

Publication Date

2015-08-01

DOI

10.1002/ijc.29415

Peer reviewed

Antitumor activity of an anti-CD98 antibody

Gregory M. Hayes¹, Lawrence Chinn¹, Joseph M. Cantor², Belinda Cairns¹, Zoia Levashova¹, Hoang Tran¹, Timothy Velilla¹, Dana Duey¹, John Lippincott¹, Joseph Zachwieja¹, Mark H. Ginsberg² and Edward H. van der Horst¹

¹Pre-Clinical Development, Igenica Biotherapeutics, CA

²School of Medicine, University of California—San Diego, La Jolla, CA

CD98 is expressed on several tissue types and specifically upregulated on fast-cycling cells undergoing clonal expansion. Various solid (e.g., nonsmall cell lung carcinoma) as well as hematological malignancies (e.g., acute myeloid leukemia) overexpress CD98. We have identified a CD98-specific mouse monoclonal antibody that exhibits potent preclinical antitumor activity against established lymphoma tumor xenografts. Additionally, the humanized antibody designated IGN523 demonstrated robust tumor growth inhibition in leukemic cell-line derived xenograft models and was as efficacious as standard of care carboplatin in patient-derived nonsmall lung cancer xenografts. *In vitro* studies revealed that IGN523 elicited strong ADCC activity, induced lysosomal membrane permeabilization and inhibited essential amino acid transport function, ultimately resulting in caspase-3 and -7-mediated apoptosis of tumor cells. IGN523 is currently being evaluated in a Phase I clinical trial for acute myeloid leukemia (NCT02040506). Furthermore, preclinical data support the therapeutic potential of IGN523 in solid tumors.

CD98 is a heterodimeric protein that comprises a heavy and light chain. The CD98 heavy chain is a type II transmembrane glycoprotein that forms a heterodimer *via* covalent linkage to one of 6 amino acid transporters.^{1,2} CD98 is overexpressed on the cell surface of almost all tumor cells, regardless of tissue origin and increased expression of a CD98-light chain, L-type amino acid transporter 1 (LAT-1) occurs in many types of human cancers, including breast, colon, oral, ovarian, esophageal, glioma and leukemia.^{3,4} Increased uptake of amino acids supports the high growth rate of cancer cells by providing the building blocks for protein synthesis.^{4–6} Moreover, the higher expression of CD98 heavy chain and LAT-1 in metastatic vs. primary tumors suggests that over-expression of CD98/LAT-1 may facilitate progression and metastasis of human cancers.

Key words: phenotypic screening, anti-CD98 monoclonal antibody, multiple mechanism of action, acute myeloid leukemia, non-small cell lung cancer

Additional Supporting Information may be found in the online version of this article.

This is an open access article under the terms of the Creative Commons Attribution NonCommercial License, which permits use, distribution and reproduction in any medium, provided the original work is properly cited and is not used for commercial purposes. The copyright line for this article was changed on 15 September 2015 after original online publication.

E.H.vH, G.M.H, L.C. B.C, Z.L. and T.V. are employees of Igenica Biotherapeutics

DOI: 10.1002/ijc.29415

History: Received 15 Aug 2014; Accepted 18 Dec 2014; Online 29 Dec 2014

Correspondence to: Dr. Edward H. van der Horst, Igenica Biotherapeutics, 863 Mitten Rd, Ste. 102, Burlingame, CA 94010, USA, Tel.: +1-650-231-4325, Fax: +1-650-697-4900, E-mail: evanderhorst@igenica.com

CD98 also regulates integrin signaling by association with integrin β -subunits, thereby controlling cell proliferation, survival, migration, epithelial adhesion and polarity.^{3,7} The function of CD98 in regulating both amino acid transport and integrin signaling can contribute to the rapid proliferation and clonal expansion of lymphocytes and tumor cells.³

The expression pattern and pleiotropic function of CD98 heavy and light chains suggest these proteins are promising targets for treatment of a variety of human cancers. Although small molecule inhibitors of LAT-1 activity have demonstrated preclinical antitumor activity in a number of cancer cell types, including NSCLC, colon cancer, oral cancer and breast cancer, development of antibodies against CD98 heavy chain has received less focus.^{5,8–10} Murine monoclonal antibodies to CD98 inhibit lymphocyte proliferation and the growth of bladder cancer, lymphoma, glioma, prostate and colon cancer cells in preclinical models.^{11–13}

To identify therapeutic anti-CD98 antibodies with significant antitumor activity, we used *in vivo* phenotypic screening. The advantage of phenotypic screening for antibodies against novel targets compared with the more common target-based screening, is 2-fold.¹⁴ First, it allows for the identification of potent functional antibodies with antitumor properties *in vivo* and second, it obviates the need for prior understanding of the molecular mechanism of action (MOA). Activity in phenotypic screening is more likely to translate into therapeutic efficacy than activity in target-based assays.

Here, we describe the discovery and characterization of IGN523, a humanized monoclonal antibody targeting CD98, which possesses multiple MOAs and elicits potent *in vivo* antitumor activity in several human cancer models.

Material and Methods

General materials

Recombinant His-tagged human CD98 fusion protein was purchased from Sinobiological (Beijing, China). Antibodies

What's new?

The CD98 protein is overexpressed in a wide variety of cancers, and its expression levels show positive association with tumor progression and metastasis. Both the heavy and the light chains of CD98 are of therapeutic interest. The present study reports broad and potent anti-tumor activity of the anti-CD98 humanized monoclonal antibody IGN523 in leukemic cell-line-derived xenograft models and patient-derived non-small cell lung cancer xenografts. IGN523 exhibited multiple mechanisms of action, and *in vitro* demonstrated antibody-dependent cellular cytotoxicity, blocked amino acid transport, and led to tumor cell apoptosis mediated via caspase-3 and caspase-7 pathways.

used in flow cytometry were from Miltenyi Biotec (Cologne, Germany) and EMD Millipore (Billerica, MA), respectively. For crosslinking experiments, an anti-human Fc γ -specific polyclonal goat antibody (AbXL) was obtained from Jackson ImmunoResearch Laboratories (Westgrove, PA). Murine IgG2a antibody (clone HB-121) served as an isotype control (ATCC, Manassas, VA). Ramos (CRL-1596), HL-60 (CCL-240), KG-1 (CRL-8031) and B16-F10 (CRL-6475) were obtained from ATCC. OCI-AML-3 (ACC-582) was obtained from DMSZ (Braunschweig, Germany). Cell lines were cultured according to the suppliers' protocols. Cetuximab (Erbix, Eli Lilly, Indianapolis, IN) and rituximab (Rituxan, Genentech, South San Francisco, CA) were used as active controls where appropriate. The Cooperative Human Tissue Network (CHTN) and the National Disease Research Interchange provided primary tumor tissue samples, respectively. CHTN is funded by the National Cancer Institute.

Antibody-dependent cellular cytotoxicity (ADCC) and Complement-dependent cytotoxicity (CDC) assays

The ADCC Reporter Bioassay from Promega (Madison, WI) was used in Ramos, KG-1, OCI-AML-3 and B16-F10 according to the manufacturer's protocol. Briefly, the activation of gene transcription through the nuclear factor of activated T-cells pathway (NFAT) in the effector cells is measured. Engineered Jurkat cells stably expressing the Fc γ RIIIa receptor, V158 (high affinity) variant and an NFAT response element driving expression of firefly luciferase were used as effector cells at a ratio of 6:1 (effector to target cell ratio, E/T). ADCC is quantified through NFAT pathway induced luminescence.¹⁵ Assay equivalency was demonstrated using purified human peripheral NK cells in Ramos and KG-1 cells (Supporting Information Methods).

For CDC assays, normal human serum (10% final concentration) was added to initiate the CDC cascade. Nonlinear curve-fit (4-parameter dose-response curve fit with variable slope) was applied and data were analyzed and graphed by GraphPadPrism vers. 5.0f (GraphPad Software, La Jolla, CA).

Amino acid transport assay

Amino acid transport activity was tested following a modified protocol.¹⁶ ³H-labeled Phe (126 Ci/mM) was purchased from Perkin Elmer (Santa Clara, CA). 2-aminobicyclo[2.2.1]heptane-2-carboxylic acid (BCH) was obtained from Sigma-Aldrich (St. Louis, MO). Briefly, 2×10^5 cells were incubated with IGN523 and AbXL for 30 min prior to the addition of

³H-Phe for 2 min. Parallel cultures were treated with 10 mM BCH to serve as a positive control. Cells were washed, lysed and cell lysates mixed with scintillation fluid. Radioactivity was quantified in a Perkin Elmer 1450 MicroBeta Trilux (Santa Clara, CA).

Viability and apoptosis assays

Viability and caspase-3 and caspase-7-mediated apoptosis were quantified using the ApoTox-Glo kit provided by Promega (Madison, WI) according to the manufacturer's protocol. Cells were plated at 2×10^4 cells/well onto a 96-well plate in complete media and incubated for 24 hr. For IGN523 crosslinking studies, cells were preincubated with 2 μ g/ml IGN523 in the presence or absence of 10 μ g/ml AbXL. Cells were then incubated for 48 hr and viability and caspase-3 and caspase-7-mediated apoptosis measured.

Lysosome volume and permeability assays

LysoTracker Deep Red and acridine orange (AO) were purchased from Molecular Probes/Life Technologies (Grand Island, NY). In both assays, following lysosome labeling, Ramos cells were treated with 10 μ g/mL IGN523 in the presence or absence of 50 μ g/mL crosslinking antibody for 30 min at 37 °C. Assessment of lysosomal volume and permeability was performed as described previously, with 3×10^6 cells labeled either with 50 nM LysoTracker Deep Red for 1 hr or with 5 μ M acridine orange (AO) for 15 min at 37 °C.¹⁷ AO is a metachromatic fluorochrome that emits red fluorescence when highly concentrated in acidic lysosomes and emits green fluorescence in the more pH neutral cytosol. Leakage of lysosomal contents into the cytosol can be detected as an increase in green fluorescence by flow cytometry.

Flow cytometry

Flow cytometric data were acquired using a MACSQuant Analyzer 10 cytometer (Miltenyi Biotec, Cologne, Germany) operated by MACSQuantify software and at least 30,000 viable events were collected per sample. Data was analyzed using FlowJo software (Version 10.0.7, Tree Star, Ashland, OR).

Immunofluorescence

Ramos cells were incubated at 4 °C for 30 min with 2 μ g/mL Alexa488-labeled IGN523 in the presence or absence of 10 μ g/mL crosslinking antibody and Hoechst (Life Technologies). Cells were subsequently incubated at 37 °C for the indicated time points (0–90 min) before being fixed with an

equal volume of ice cold 10% phosphate-buffered formalin. Fixed cells were cytospun, stained with 0.2 µg/mL anti-human LAMP1 (BD Pharmingen, San Jose, CA) and mounted with ProLong Gold reagent (Life Technologies). Images were taken using an IX51 microscope (Olympus, Center Valley, PA) operated by MetaMorph imaging software (Molecular Devices, Sunnyvale, CA).

Xenograft transplantation experiments

Patient-derived tumor tissue was passaged *in vivo* as described previously.¹⁸ IGN-LNG-12 and -54 are proprietary patient-derived lung tumor xenograft lines that were established at Igenica Biotherapeutics. IGN-LNG-12 is a metastatic poorly differentiated (Grade 3) NSCLC. IGN-LNG-54 is a moderately differentiated (Grade 2) NSCLC. Immunocompromised female NOD/SCID mice were used for the establishment of IGN-LNG-12, IGN-LNG-54 and KG-1 tumor xenografts, and female CB17-SCID (Swiss CD-1) mice were used for the Ramos, HL-60 and OCI-AML-3 tumor models (Charles River, Wilmington, MA). Mice were subcutaneously injected on the right flank with 1×10^6 (IGN-LNG-12 and IGN-LNG-54) or at least 1×10^7 viable cells (Ramos, HL-60, OCI-AML-3, KG-1). When the tumor reached a size between 65 and 300 mm³, mice were randomized to treatment. Antibodies were administered weekly, or as indicated, and tumors measured twice weekly. Tumor volume was calculated using the modified ellipsoid formula $\pi/6(\text{Length} \times \text{Width}^2)$. All experiments were performed on groups of at least eight animals per group. Animal experiments were performed in accordance with protocols approved by the Igenica Biotherapeutics Institutional Review Board—Animal Care and Use Committee.

Statistical analysis

Data are either expressed as the mean \pm standard error of the mean *in vivo*, or \pm the standard deviation, *in vitro*. Group means were compared using Student's 2-tailed, unpaired *t* test. Probability (*p*) values of <0.05 were interpreted as significantly different and not adjusted for multiple comparisons. All statistical analyses were performed using Microsoft EXCEL (Microsoft, Redmond, WA) and GraphPad Prism v.5.0f (GraphPad Software).

Additional and more detailed experimental procedures are provided in Supporting Information Methods.

Results

Phenotypic *in vivo* screening identifies anti-CD98 antibody that strongly inhibits tumor growth

Expression analysis of CD98 in primary AML cells and NSCLC samples, revealed that it was overexpressed in $>90\%$ of AML patients and approximately 55% of patients with the squamous cell carcinoma subtype of NSCLC (Supporting Information Figs. S1a and S1b). Consequently, we generated human CD98-specific murine monoclonal antibodies (mAbs), using Igenica's cell-based *in vivo* immunization approach

followed by standard hybridoma technology.¹⁹ After isotype analysis, verification of antigen specificity and epitope binning, 19 mAbs were evaluated for antitumor activity by assessing their impact on the growth of established heterotopic human tumors in immunodeficient mice.¹⁹ First, the mAbs were tested in the CD98-positive Ramos Burkitt's lymphoma model (Fig. 1a; Supporting Information Fig. S1c). In 3 iterations of *in vivo* screening, antibody 18-2A consistently demonstrated potent antitumor activity that was higher than the standard of care, rituximab. 18-2A was then evaluated in the CD98-positive Dau Burkitt's lymphoma model where it showed tumor growth inhibition (TGI) of 48% ($p < 0.01$; Supporting Information Fig. S1d). Based on its robust antitumor activity *in vivo*, 18-2A was selected for humanization.

Humanized anti-CD98 antibody IGN523 inhibits tumor growth of various cancers

To verify antibody-antigen binding affinities and biological activity were retained after the humanization process, the binding characteristics of both 18-2A and IGN523, the humanized version of 18-2A, were assessed by surface plasmon resonance and biological activity tested *in vivo*. The k_{on} , k_{off} and K_D values of 18-2A and IGN523 were nearly identical, indicating that the binding affinity toward human CD98 had been retained (Fig. 1b).

Tumor growth inhibitory characteristics were compared between 18-2A and IGN523 by treating established Ramos and Dau xenografts (Figs. 1c and 1d). The TGI of 18-2A and IGN523 were very similar in Ramos (92% vs. 98%, respectively) and slightly higher for IGN523 in DAU (76% vs. 43%), suggesting that the antitumor properties of 18-2A were also retained.

Because CD98 is highly expressed across many malignancies, we evaluated IGN523 in a range of established CD98-positive xenograft cancer models. IGN523 was tested in the AML models HL-60, OCI-AML-3 and KG-1, and in 2 patient-derived NSCLC xenograft models, IGN-LNG-12 and IGN-LNG-54 (Fig. 2). IGN523 was also compared with the standard of care drug carboplatin in the NSCLC xenograft models (Figs. 2d and 2e). IGN523 significantly reduced tumor growth compared with isotype control in all 5 xenograft models: HL-60 (94%, $p < 0.001$), OCI-AML-3 (74%, $p < 0.001$), KG-1 (53%, $p < 0.05$), IGN-LNG-12 (44%, $p < 0.001$) and IGN-LNG-54 (56%, $p < 0.001$). Notably, although carboplatin at its maximal tolerated dose produced a significant TGI in IGN-LNG-12 (44%, $p < 0.001$) and IGN-LNG-54 (31%, $p < 0.05$), it also resulted in toxicity as evidenced by marked body weight loss (17.6 ± 1.3 g final weight in IGN-LNG-12; 22.2 ± 2.4 g final weight in IGN-LNG-54; Supporting Information Fig. S2). In contrast, IGN523 treatment exerted comparable or higher antitumor effect compared with carboplatin (56% vs. 31% in IGN-LNG-54, $p = 0.04$), without inducing body weight loss (20.1 ± 1.8 g final weight in IGN-LNG-12; 25.6 ± 2 g final weight in IGN-LNG-54). These data demonstrate that IGN523

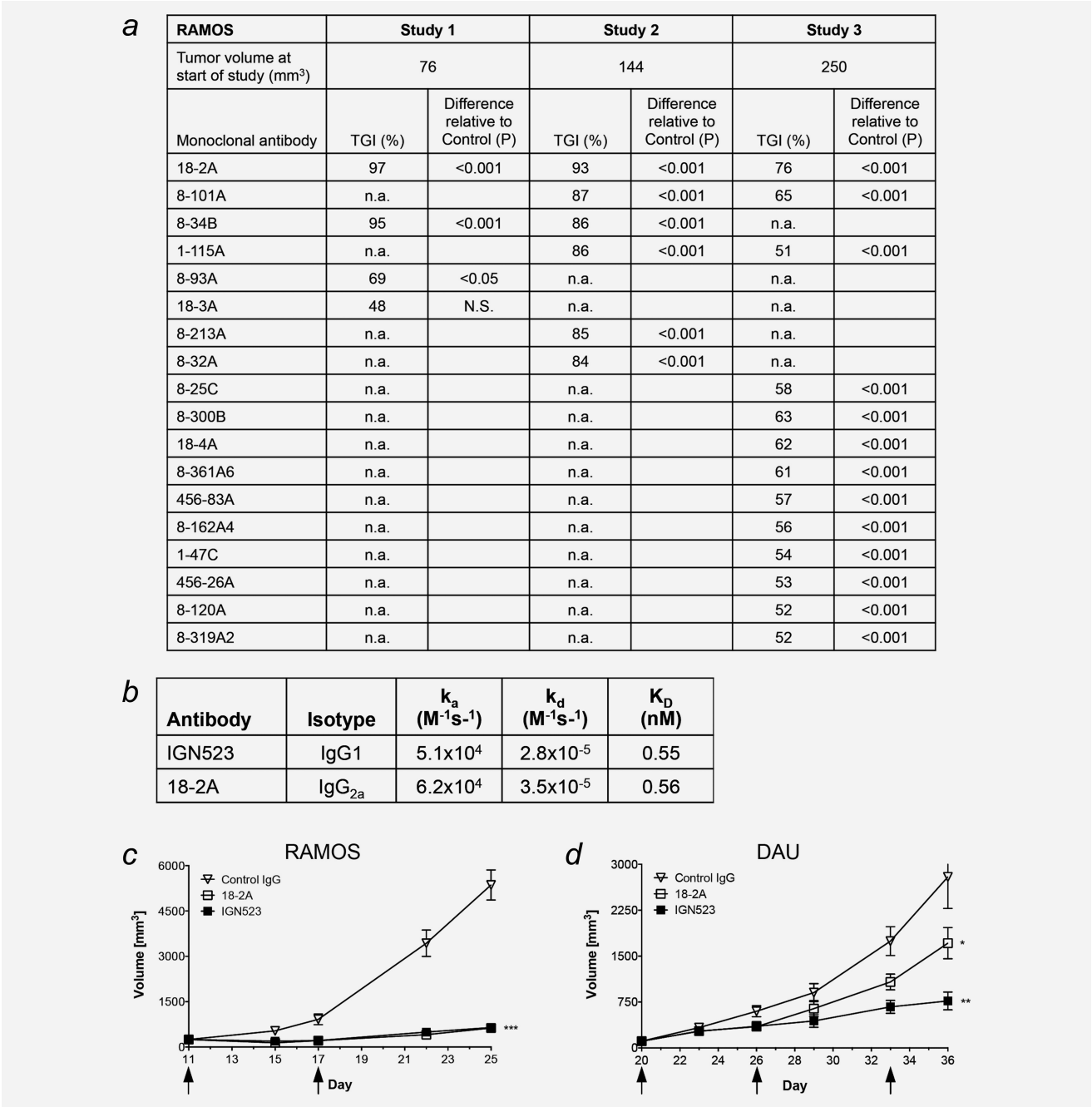


Figure 1. Antitumor activity of anti-CD98 antibodies in Burkitt’s lymphoma model ramos, biophysical properties of 18-2A and IGN523 and comparison of their antitumor efficacy in ramos and dau Burkitt’s lymphoma xenografts. (a) of note, in studies 1 and 2, rituximab was used as a positive control and elicited a TGI of 88% ($p < 0.001$) and 68% ($p < 0.001$), respectively. (b) biacore analysis of 18-2A (murine IgG_{2a}) and IGN523 (human IgG1) on recombinant human CD98 protein. (c) ramos or (d) dau growth curves in mice receiving 18-2A (15 mg/kg), IGN523 (15 mg/kg) or control antibody (control IgG; 15 mg/kg) once weekly intraperitoneally (i.p.) ($n = 8$); (c) *** $p < 0.001$ versus control, (d) * $p < 0.05$; ** $p < 0.01$ relative to control. Treatment started on day of randomization. Starting tumor volumes were 248 ± 112 and 111 ± 38 mm³ for ramos and dau, respectively. Please note no statistical difference between 18-2A and IGN523 treatment groups in ramos. Arrow = administration of antibody; N.S. = statistically not significant; n.a. = not applicable.

treatment is as effective as carboplatin without inducing body weight loss in NOD/SCID mice.

In addition to measuring TGI, CD98 expression was examined in the patient-derived xenografts by staining tumor tissue sections with a polyclonal rabbit anti-CD98 antibody

post-treatment (Fig. 2f). CD98 expression was completely abrogated in the IGN523 treatment group, while CD98 levels were unchanged in the control and carboplatin treatment groups. This suggests that IGN523-mediated down regulation of CD98 led to elimination of CD98⁺-tumor cells.

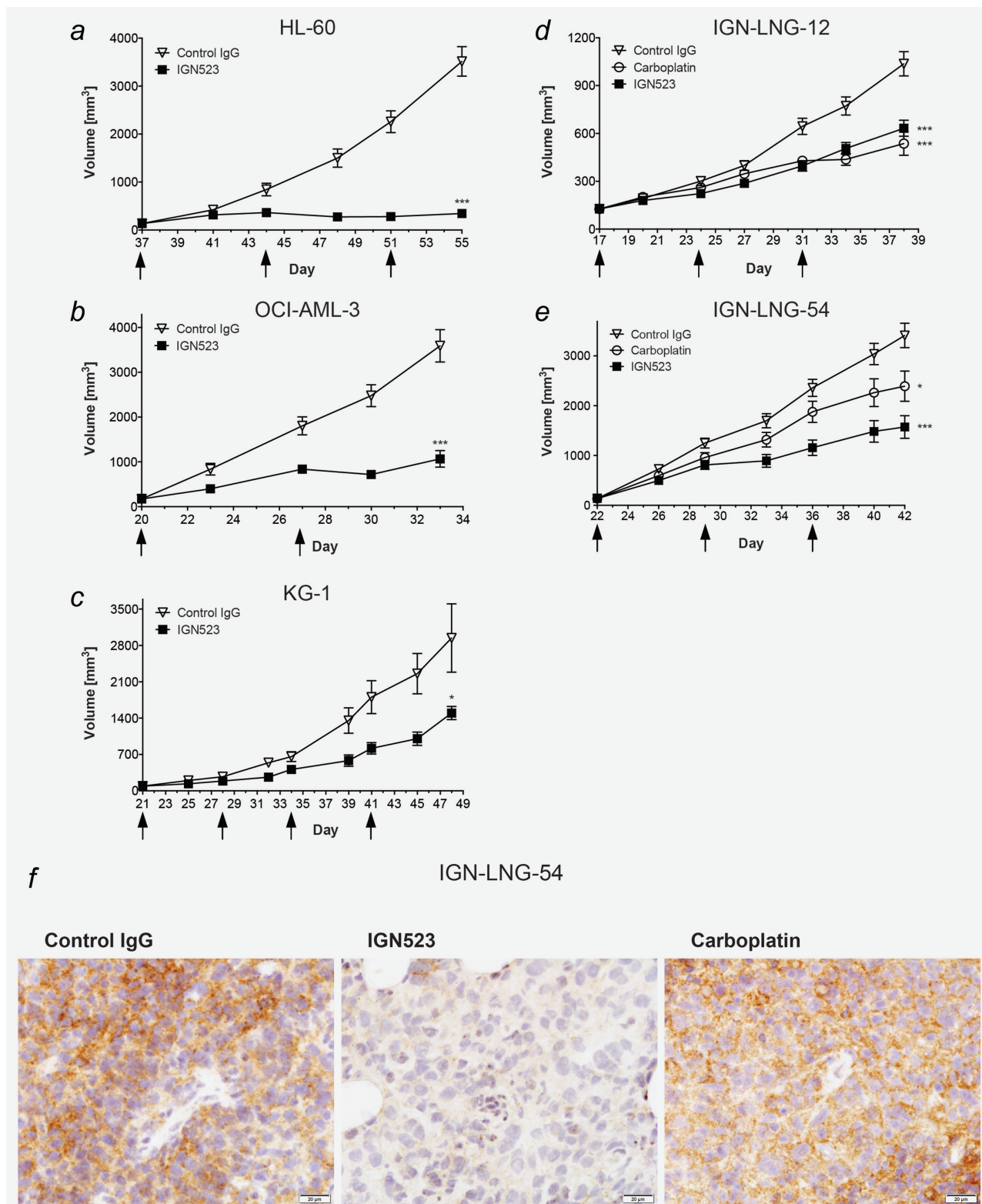


Figure 2. Tumor growth inhibition of IGN523 in different tumor models. (a) HL-60, (b) OCI-AML-3, (c) KG-1, (d) IGN-LNG-12 and (e) IGN-LNG-54 growth curves in either NOD/SCID- (c–e) or CB.17-SCID-mice (a and b) receiving IGN523 (15 mg/kg) or control IgG (15 mg/kg). Carboplatin was administered in IGN-LNG-12 and IGN-LNG-54 at 10 mg/kg i.p. ($n = 8$). (f) anti-CD98 staining of representative IGN-LNG-54 tumors post-treatment. * $p < 0.05$; *** $p < 0.001$ relative to control. Starting tumor volumes were 134 ± 32 mm³ (HL-60); 174 ± 34 mm³ (OCI-AML-3); 92 ± 11 mm³ (KG-1); 126 ± 23 mm³ (IGN-LNG-12) and 136 ± 38 mm³ (IGN-LNG-54). Please note a statistical difference between IGN523 and carboplatin treatment groups in IGN-LNG-54 ($p < 0.04$). Arrow = administration of antibody. Scale bar = 20 μ m.

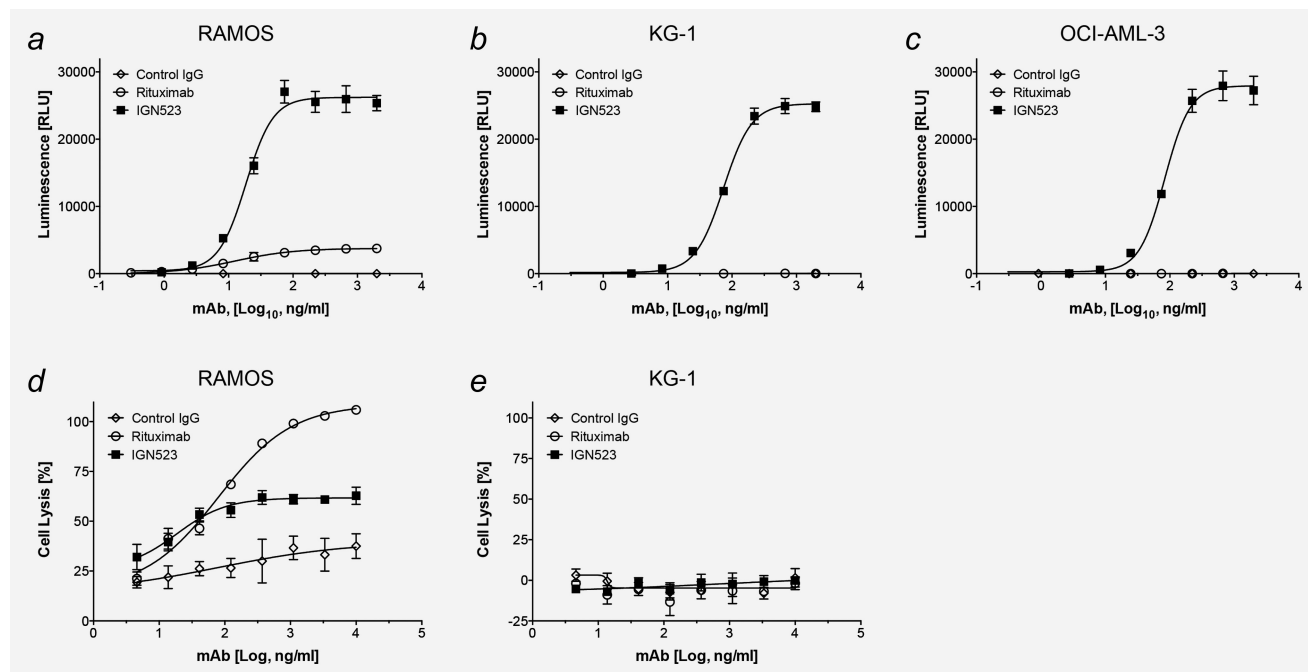


Figure 3. IGN523 demonstrates strong ADCC-, but not CDC-activity. Antibody-induced luciferase activity in the effector cell is quantified with luminescence readout and is a surrogate for effector cell-mediated cell lysis. Target cells (a and d) Ramos, (b and e) KG-1 and (c) OCI-AML-3 were used in (a–c) ADCC or (d and e) CDC assays. Please note that IGN523 elicits greater ADCC activity than rituximab in Ramos cells. Cetuximab (anti-EGFR) was used as negative control antibody (control IgG). Ramos, KG-1 and OCI-AML-3 cell lines both endogenously express CD98 on the cell surface.

In summary, the humanized anti-CD98 antibody IGN523 maintained both the binding affinity and biological activity of its parental antibody. IGN523 inhibited tumor growth in AML and primary NSCLC xenograft models.

IGN523 elicits strong Antibody-dependent cellular cytotoxicity, but not Complement-dependent cytotoxicity

ADCC and CDC are clinically relevant MOAs for therapeutic antibodies, e.g., rituximab (anti-CD20).²⁰ Consequently, ADCC and CDC induction by IGN523 was evaluated (Fig. 3). Ramos, KG-1 and OCI-AML-3 cells were used as target cells, because they were sensitive to IGN523 treatment *in vivo*. Rituximab and cetuximab (anti-EGFR) served as control biologics in these evaluations. The EC₅₀ data demonstrated that IGN523 elicited strong ADCC activity at 18.6 ng/mL, 73.8 ng/mL and 83.3 ng/mL in Ramos, KG-1 or OCI-AML-3 cells, respectively (Figs. 3a–3c) and a significantly greater ADCC activity in CD98⁺- and CD20⁺-Ramos cells than rituximab. IGN523 did not produce CDC activity in KG-1 cells and elicited only marginal CDC activity at 12 ng/mL in Ramos cells (Figs. 3d and 3e). As a negative control we used the mouse melanoma cell line B16-F10 and did not observe IGN523-induced ADCC activity, since IGN523 specifically binds to human CD98 (Supporting Information Fig. S4a). Therefore, ADCC is likely a contributing mechanism for antitumor activity of IGN523, while CDC appears less important.

IGN523 elicits Caspase-dependent apoptosis, increases lysosomal membrane permeability and decreases amino acid transport

Another mechanism by which antibodies may exert antitumor activity is receptor crosslinking on the cell surface.²¹ For example, anti-CD20 antibody rituximab, initiates the mitochondrial apoptosis pathway, which does not necessarily require active caspases.²² Antibody crosslinking by immune cells expressing Fcγ-receptors such as leukocytes can be therapeutically beneficial by triggering pro-apoptotic stimuli in cancer cells.²¹ This effect can be mimicked *in vitro* by using an anti-Fc antibody, such as a polyclonal goat anti-human IgG, AbXL.

To investigate the potential relationship between anti-IGN523 crosslinking and tumor cell viability, Ramos, OCI-AML-3 and KG-1 cells were treated with IGN523 in the presence or absence of AbXL and assessed for survival (Figs. 4a–4c). Measuring the protease activity restricted to intact viable cells revealed that IGN523 treatment substantially decreased cell viability in the presence of AbXL (Ramos: 70% reduction, $p < 0.001$; OCI-AML-3: 76% reduction, $p < 0.001$; KG-1: 80% reduction, $p < 0.001$), but not when used alone. A concomitant increase in caspase-3 and caspase-7 activity indicated that the IGN523-induced cell death was caspase-mediated (Ramos: 3.3-fold, $p < 0.001$; OCI-AML-3: 7.5-fold, $p < 0.001$ and KG-1: 6.6-fold, $p < 0.001$; Figs. 4d–4f).

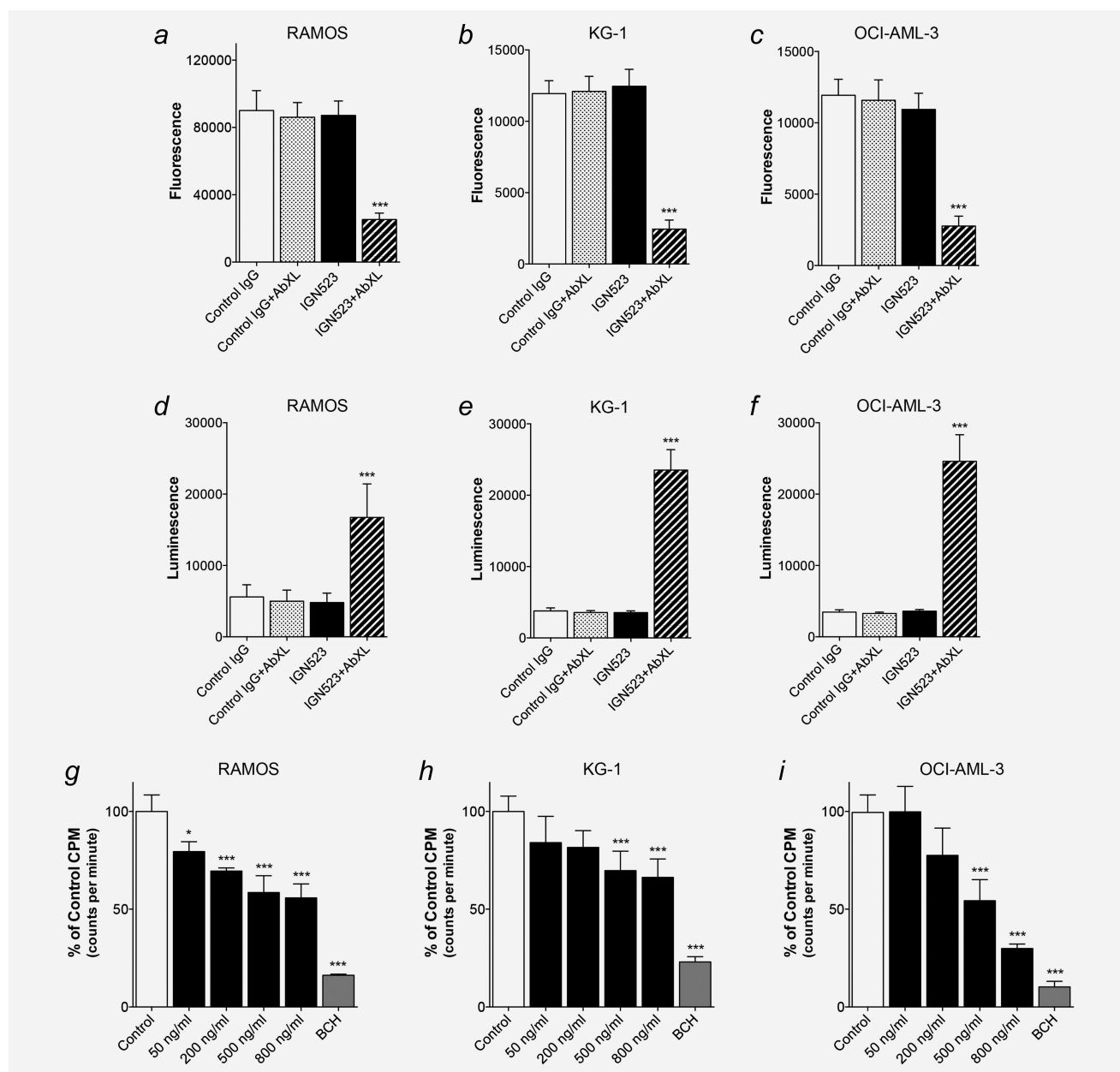


Figure 4. IGN523 decreases viability, amino acid transport and increases caspase-3 and caspase-7 activity. Cells were incubated with IGN523 in the presence or absence of AbXL. (a–c) cell viability was assessed by measurement of live-cell protease activity that is restricted to intact viable cells (fluorescence). (d–f) Caspase-3 and caspase-7 activity was measured by increase in aminoluciferin-induced luminescence through DEVD-aminoluciferin substrate cleavage. (g–i) crosslinked IGN523 reduced ^3Phe -uptake. BCH was used at 10 mM. The ratio of IGN523:AbXL was 1:5. The amount of ^3Phe -uptake in ramos cells under each treatment determined as counts per minute (cpm) is graphed. * $p < 0.05$; *** $p < 0.001$ relative to IGN523 (a and b) or control (c), respectively.

CD98 heavy chain serves as a dimerization partner for any of 6 light chain amino acid transporters, whose functional activity depends on the presence of the heavy chain.²³ Since impairment of amino acid exchange can impair cancer cell growth, the impact of IGN523 upon cellular import of essential amino acids was investigated in Ramos, OCI-AML-3 and KG-1 cells (Figs. 4g–4i). The cells were treated with IGN523 plus AbXL prior to incubation with ^3H -phenylalanine. In parallel, cells were treated with 10 mM 2-aminobicyclo[2.2.1]-

heptane-2-carboxylic acid (BCH), a nonmetabolizable leucine analogue and inhibitor of the large neutral amino acid transporters LAT-1 and LAT-2,²⁴ as a control. Crosslinking of CD98 resulted in a significant reduction of labeled phenylalanine by 20–44% (Ramos), 45–70% (OCI-AML-3) and 30–34% (KG-1), respectively, indicating that IGN523-crosslinking reduced the transport of this essential amino acid. As a specificity control we again used the mouse melanoma cell line B16-F10 and did not observe IGN523-mediated decrease in

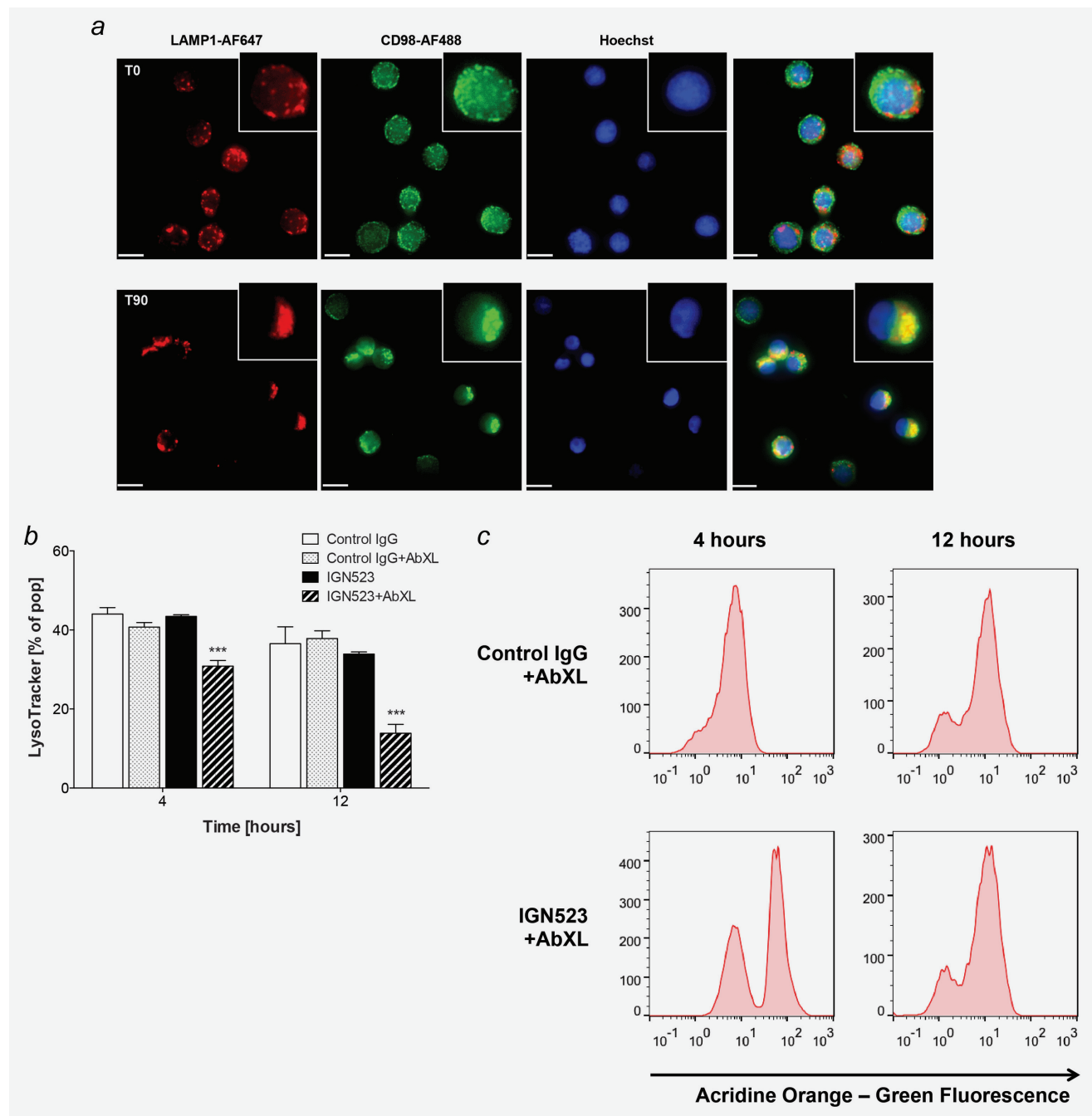


Figure 5. IG523-CD98 complex colocalizes with LAMP-1. IG523 induces lysosomal permeability. (a) ramos cells were incubated at 4 °C for 30 min with 2 µg/mL Alexa488-labeled anti-human CD98 antibody (green), 10 µg/mL anti-human crosslinker (AbXL) and hoechst (blue). Cells were subsequently incubated at 37 °C for the indicated time points (0 or 90 min). LAMP1 was stained with anti-LAMP1-AF647 antibody (red). Note that CD98 and LAMP-1 colocalize (yellow). Top row: 0 min; bottom row: 90 min; scale bar = 10 µm. (b) lysosomal volume and (c) lysosomal permeability was assessed in IG523-crosslinked ramos cells at 4 and 12 hr, respectively. The ratio of IG523 (10 µg/mL):AbXL (50µg/mL) was 1:5. Cetuximab was used as control antibody (control IgG). ****p* < 0.001 relative to IG523.

cell viability, increase in caspase activity or decrease in amino acid transport, respectively (Figs. S4b–S4d).

Enhanced ADCC activity, as well as increased lysosomal membrane permeabilization (LMP), has been demonstrated with crosslinked CD20.²⁵ To assess whether similar effects are seen with IG523 plus crosslinker, we investigated if the

CD98-IG523 complex was internalized to lysosomes and whether this led to increased lysosomal permeability (Fig. 5). Immunofluorescence studies of IG523-treated Ramos cells in the presence or absence of AbXL showed that the CD98-IG523 complex localized to lysosome-associated membrane protein LAMP-1 structures and that the rate of internalization

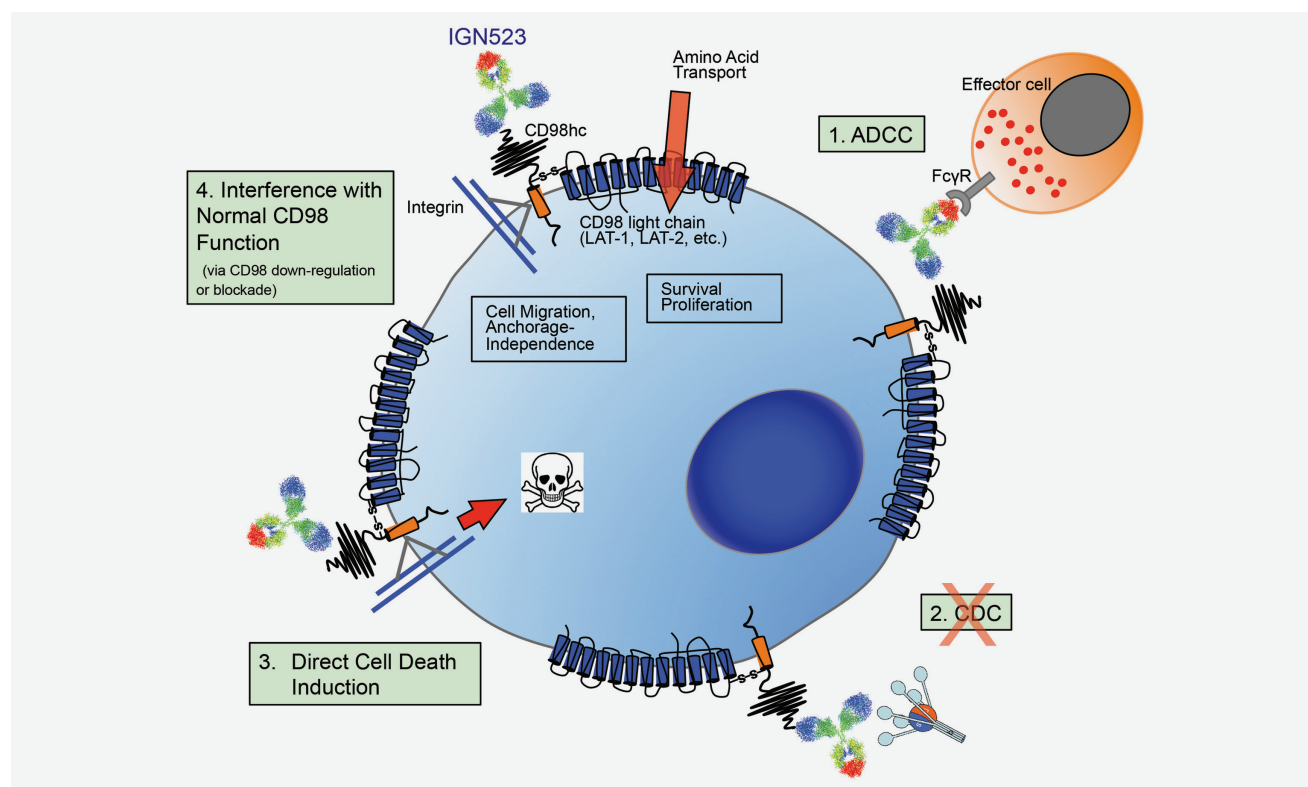


Figure 6. Mechanisms of action for IGN523. IGN523 encompasses multiple, diverse mechanisms of action. *In vitro* analysis of IGN523 upon multiple tumor cells demonstrates a potent ADCC ability for this antibody. Crosslinking of IGN523 upon tumor cells significantly reduces both the import of essential amino acids and increases lysosomal membrane permeability. Together, these MOAs resulted in caspase-3 and caspase-7 activation and cell death.

was increased by crosslinking. Moreover, in the presence of IGN523, CD98 seemed to be capped at the cell surface. This is reminiscent of the CD20 distribution with rituximab treatment that augments NK-cell-mediated ADCC²⁶ (Fig. 5a).

We next determined whether lysosomal integrity was impaired after internalization of the CD98-antibody complex. Following IGN523 incubation and addition of AbXL, Ramos cells were harvested and assessed for changes in lysosomal volume and permeability *via* flow cytometry (Figs. 5b and 5c). Treatment with IGN523 and AbXL decreased the LysoTracker-positive population by 60 and 77% at 12 and 24 hr, respectively, suggesting an induction of lysosomal collapse (Fig. 5b). LMP was assessed by measuring the increase in green fluorescence that occurs when AO-labeled lysosomes leak into the cytosol¹⁷ (Fig. 5c). IGN523 increased AO green fluorescence within 4 hr after treatment, indicating LMP. This was followed by a decrease in green fluorescence at 12 hr. Taken together, these data suggest the CD98-IGN523 complex is efficiently internalized and shuttled to lysosomes. Moreover, IGN523 in the presence of AbXL decreases lysosomal integrity and reduces amino acid transport resulting in cell death.

Discussion

The presence of CD98 on cancer cells is well established: it is expressed on a wide variety of solid and hematological

malignancies, and its overexpression correlates with both poor prognosis and cellular transformation (reviewed in Refs. 3, 27). This study describes the antitumor activity of IGN523, a humanized antibody against CD98. Phenotypic screening *in vivo* enabled identification of an antibody with therapeutic potential based on tumor growth inhibition, without detailed *a priori* knowledge of its mechanism of action. A recent analysis noted that phenotypic drug discovery strategies were more successful for first-in-class medicines, whereas target-based molecular strategies were more successful for follow-on drugs.¹⁴ Phenotypic screening was successful for IGN523, the first anti-CD98 antibody to enter into clinical trial for AML (NCT02040506).

Subsequent studies investigated the mechanisms of IG523 action. Important mechanisms responsible for the therapeutic benefit of monoclonal antibodies in oncology include strong ADCC activity and signal perturbation of cancer-relevant pathways, although the role of CDC remains unclear.^{20,28} Because drug resistance mechanisms in cancer treatment lead to poor patient outcomes, targeting several orthogonal pathways with different drugs or using a drug with multiple mechanisms of action may delay or overcome drug resistance.²⁹ Therapeutic anti-CD20 antibodies, such as rituximab and obinutuzumab, elicit ADCC. In addition to ADCC induction, rituximab-mediated capping of CD20 has been

proposed as an additional MOA, enhancing NK-mediated cytotoxicity.²⁶ Obinutuzumab not only possesses ADCC activity, but also exhibits multiple MOAs *in vitro*, including enhanced noncaspase-dependent induction of direct cell death.²⁵

Similarly, IGN523 possesses multiple mechanisms of action, as shown here in several cell lines *in vitro* (Fig. 6). First, the ADCC activity of IGN523 against Ramos, OCI-AML-3 and KG-1 cells is robust. The data suggest that IGN523 may also concentrate CD98 on the target cell surface, possibly inducing a more potent ADCC activity *in vivo* through enhanced NK-recruitment. Second, in these cell lines, IGN523 elicits caspase-3 and caspase-7 mediated apoptosis in the presence of crosslinking antibody. Third, IGN523 inhibits the uptake of the essential amino acid phenylalanine *in vitro*. Lastly, CD98-IGN523 complex colocalized with LAMP-1 and led to increased lysosomal permeability. As with anti-CD20 antibodies, crosslinking antibody *in vitro* that simulates immune cells expressing Fcγ-receptors *in vivo*, enables additional cytotoxic actions for IGN523, but with different involvement of caspases compared with the anti-CD20 antibodies.

Targeting cancer metabolism has emerged as a promising therapeutic approach, due to the increased metabolic demands of cancer cells.⁶ Recent studies have shown that L-asparaginase depletion of glutamine profoundly inhibits protein synthesis and produces a strong apoptotic response in primary AML cells.³⁰ Importantly, CD98 is the main heterodimerization partner for 6 amino acid transporters, which are dependent on

the CD98 heavy chain for their localization and proper function.²³ Among those 6 transporters, the bi-directional transporters LAT-1 and LAT-2 export nonessential glutamine to enable the uptake of essential amino acids, which in turn activate the mammalian target of the rapamycin pathway promoting cell growth and survival.³¹ Although biologically active small molecules against CD98-associated light chains have been identified, anti-CD98 antibodies provide another approach to modifying amino acid transport.^{5,11–13}

Our data demonstrate for the first time that CD98 is overexpressed in CD34⁺-primary AML cells and in the squamous cell carcinoma subtype of NSCLC (Supporting Information Figs. S1a and S1b). The overexpression on primary AML cells is an important finding, since monoclonal antibody therapies, which have been successful treatments for other hematological malignancies such as CLL,³² have heretofore not been successful for AML.

We have shown that IGN523 has potent antitumor activity across a variety of malignancies *in vivo*. The range of antitumor mechanisms exhibited by IGN523 may reduce the emergence of treatment-resistant cancer clones and improve patient outcomes. The therapeutic potential of IGN523 is currently being evaluated in clinical trials with AML patients (NCT02040506).

Acknowledgements

The authors would like to thank William Ho, Mary Haak-Frendscho and Sally Bolmer for their valuable help preparing this manuscript.

References

1. Parmacek MS, Karpinski BA, Gottesdiener KM, et al. Structure, expression and regulation of the murine 4F2 heavy chain. *Nucleic Acids Res* 1989; 17:1915–31.
2. Deves R, Boyd CA. Surface antigen CD98(4F2): not a single membrane protein, but a family of proteins with multiple functions. *J Membr Biol* 2000;173:165–77.
3. Cantor JM, Ginsberg MH. CD98 at the crossroads of adaptive immunity and cancer. *J Cell Sci* 2012;125:1373–82.
4. Fan X, Ross DD, Arakawa H, et al. Impact of system L amino acid transporter 1 (LAT1) on proliferation of human ovarian cancer cells: a possible target for combination therapy with anti-proliferative aminopeptidase inhibitors. *Biochem Pharmacol* 2010;80:811–8.
5. Imai H, Kaira K, Oriuchi N, et al. Inhibition of L-type amino acid transporter 1 has antitumor activity in non-small cell lung cancer. *Anticancer Res* 2010;30:4819–28.
6. Vander Heiden MG, Cantley LC, Thompson CB. Understanding the warburg effect: the metabolic requirements of cell proliferation. *Science (New York, NY)* 2009;324:1029–33.
7. Cai S, Bulus N, Fonseca-Siesser PM, et al. CD98 modulates integrin beta1 function in polarized epithelial cells. *J Cell Sci* 2005;118: 889–99.
8. Oda K, Hosoda N, Endo H, et al. L-type amino acid transporter 1 inhibitors inhibit tumor cell growth. *Cancer Sci* 2010;101:173–9.
9. Kim CS, Moon IS, Park JH, et al. Inhibition of L-type amino acid transporter modulates the expression of cell cycle regulatory factors in KB oral cancer cells. *Biol Pharm Bull* 2010;33: 1117–21.
10. Shennan. Inhibition of system L (LAT1/CD98hc) reduces the growth of cultured human breast cancer cells. *Oncol Rep* 1994;20:885–9.
11. Yagita H, Masuko T, Hashimoto Y. Inhibition of tumor cell growth in vitro by murine monoclonal antibodies that recognize a proliferation-associated cell surface antigen system in rats and humans. *Cancer Res* 1986;46:1478–84.
12. Yagita H, Masuko T, Takahashi N, et al. Monoclonal antibodies that inhibit activation and proliferation of lymphocytes. I. Expression of the antigen on monocytes and activated lymphocytes. *J Immunol* 1986;136:2055–61.
13. Papetti M, Herman IM. Controlling tumor-derived and vascular endothelial cell growth: role of the 4F2 cell surface antigen. *Am J Pathol* 2001;159:165–78.
14. Swinney DC, Anthony J. How were new medicines discovered? *Nat Rev Drug Discov* 2011;10: 507–19.
15. Parekh BS, Berger E, Sibley S, et al. Development and validation of an antibody-dependent cell-mediated cytotoxicity-reporter gene assay. *mAbs* 2012;4:310–8.
16. Fenczik CA, Zent R, Dellos M, et al. Distinct domains of CD98hc regulate integrins and amino acid transport. *J Biol Chem* 2001;276:8746–52.
17. Nylandsted J, Gyrd-Hansen M, Danielewicz A, et al. Heat shock protein 70 promotes cell survival by inhibiting lysosomal membrane permeabilization. *J Exp Med* 2004;200:425–35.
18. van der Horst EH, Chinn L, Wang M, et al. Discovery of fully human anti-MET monoclonal antibodies with antitumor activity against colon cancer tumor models in vivo. *Neoplasia* 2009;11: 355–64.
19. Liao-Chan S, Zachwieja J, Gomez S, et al. Monoclonal antibody binding-site diversity assessment with a cell-based clustering assay. *J Immunol Methods* 2014;405:1–14.
20. Strome SE, Sausville EA, Mann D. A mechanistic perspective of monoclonal antibodies in cancer therapy beyond target-related effects. *The Oncologist* 2007;12:1084–95.
21. Wilson NS, Yang B, Yang A, et al. An fcγ receptor-dependent mechanism drives antibody-mediated target-receptor signaling in cancer cells. *Cancer cell* 2011;19:101–13.
22. van der Kolk LE, Evers LM, Omene C, et al. CD20-induced B cell death can bypass mitochondria and caspase activation. *Leukemia* 2002;16: 1735–44.
23. Mastroberardino L, Spindler B, Pfeiffer R, et al. Amino-acid transport by heterodimers of 4F2hc/CD98 and members of a permease family. *Nature* 1998;395:288–91.
24. Wagner CA, Lang F, Broer S. Function and structure of heterodimeric amino acid transporters. *Am J Physiol Cell Physiol* 2001;281:C1077–93.

25. Alduaij W, Ivanov A, Honeychurch J, et al. Novel type II anti-CD20 monoclonal antibody (GA101) evokes homotypic adhesion and actin-dependent, lysosome-mediated cell death in B-cell malignancies. *Blood* 2011;117:4519–29.
26. Rudnicka D, Oszmiana A, Finch DK, et al. Rituximab causes a polarization of B cells that augments its therapeutic function in NK-cell-mediated antibody-dependent cellular cytotoxicity. *Blood* 2013;121:4694–702.
27. Hara K, Kudoh H, Enomoto T, et al. Malignant transformation of NIH3T3 cells by overexpression of early lymphocyte activation antigen CD98. *Biochem Biophys Res Commun* 1999;262:720–5.
28. Sliwkowski MX, Mellman I. Antibody therapeutics in cancer. *Science (New York, NY)* 2013;341:1192–8.
29. Holohan C, Van Schaeybroeck S, Longley DB, et al. Cancer drug resistance: an evolving paradigm. *Nat Rev Cancer* 2013;13:714–26.
30. Willems L, Jacque N, Jacquel A, et al. Inhibiting glutamine uptake represents an attractive new strategy for treating acute myeloid leukemia. *Blood* 2013;122:3521–32.
31. Nicklin P, Bergman P, Zhang B, et al. Bidirectional transport of amino acids regulates mTOR and autophagy. *Cell* 2009;136:521–34.
32. Ben-Kasus T, Schechter B, Sela M, et al. Cancer therapeutic antibodies come of age: targeting minimal residual disease. *Mol Oncol* 2007;1:42–54.